ANALYSIS OF NAPTF TRAFFIC TEST DATA FOR THE FIRST-YEAR RIGID PAVEMENT TEST ITEMS

By:
Edward H. Guo
Galaxy Scientific Corporation
2500 English Creek Ave.
Egg Harbor Township, NJ 08234, USA
Ph. (609) 645-0900, Fax (609) 645-2881
Edward.Guo@GalaxyScientific.com

Gordon F. Hayhoe and David R. Brill
FAA William J. Hughes Technical Center
Airport Technology R&D Branch, AAR-410
Atlantic City International Airport, NJ 08405, USA
Ph. (609) 485-8555, Fax (609) 485-4845
Gordon.Hayhoe@tc.faa.gov
David.Brill@tc.faa.gov

PRESENTED FOR THE 2002 FEDERAL AVIATION ADMINISTRATION AIRPORT TECHNOLOGY TRANSFER CONFERENCE

05/02

ABSTRACT

Three types of Portland cement concrete pavements were tested in the spring of 2000 at the Federal Aviation Administration's (FAA) National Airport Pavement Test Facility (NAPTF). These three test items were constructed on subgrades with various strengths (low, medium, and high). Traffic loads consisting of four- and six-wheel carriages at 45,000 lbs per wheel were applied on two lanes of the pavements along the longitudinal joints. After trafficking, corner cracks were observed in all three items. A total of 462 strain gages recorded the strain time history for most tests, and more than 90% of the sensors provided meaningful results. Analysis of a portion of the strain gage data that was received yielded information about when, where, and how the observed corner cracks developed. The analysis of the corner cracking is described in this paper. It is also shown that the results of the strain gage analysis are consistent with the conclusions of the visual distress survey.

PAVEMENT STRUCTURE AND LOAD LOCATIONS

Cross sections showing the structures of the three Portland cement concrete (PCC) test pavements are presented in Figure 1. Each pavement consists of fifteen 20×20 ft (6.1×6.1 m) slabs in three east-west lanes. Test pavements are designated as follows:

LRS – Low strength subgrade, Rigid pavement, Stabilized base
MRS - Medium strength subgrade, Rigid pavement, Stabilized base
HRS - High strength subgrade, Rigid pavement, Stabilized base

Figure 2 shows a plan of strain gage locations in the rigid-pavement test items. This plan is typical for all three items (LRS, MRS, and HRS). The whole test item consists of five rows of slabs in three lanes (total of 15 slabs); only slabs 2 and 3 in each lane are illustrated because only those slabs were instrumented. Typically, strain gages are located at the bottom and top of the slab at each location shown.

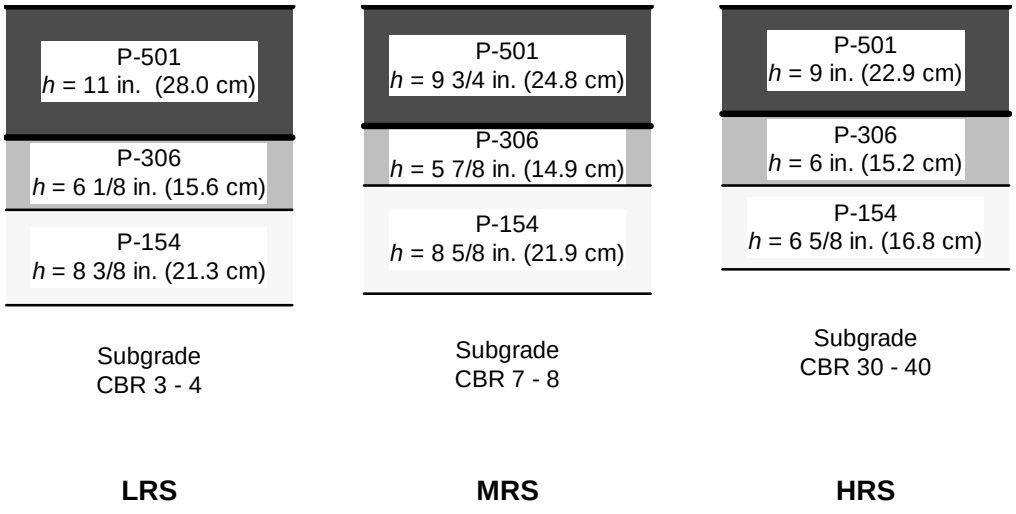

Figure 1. Cross Sections of PCC Test Items

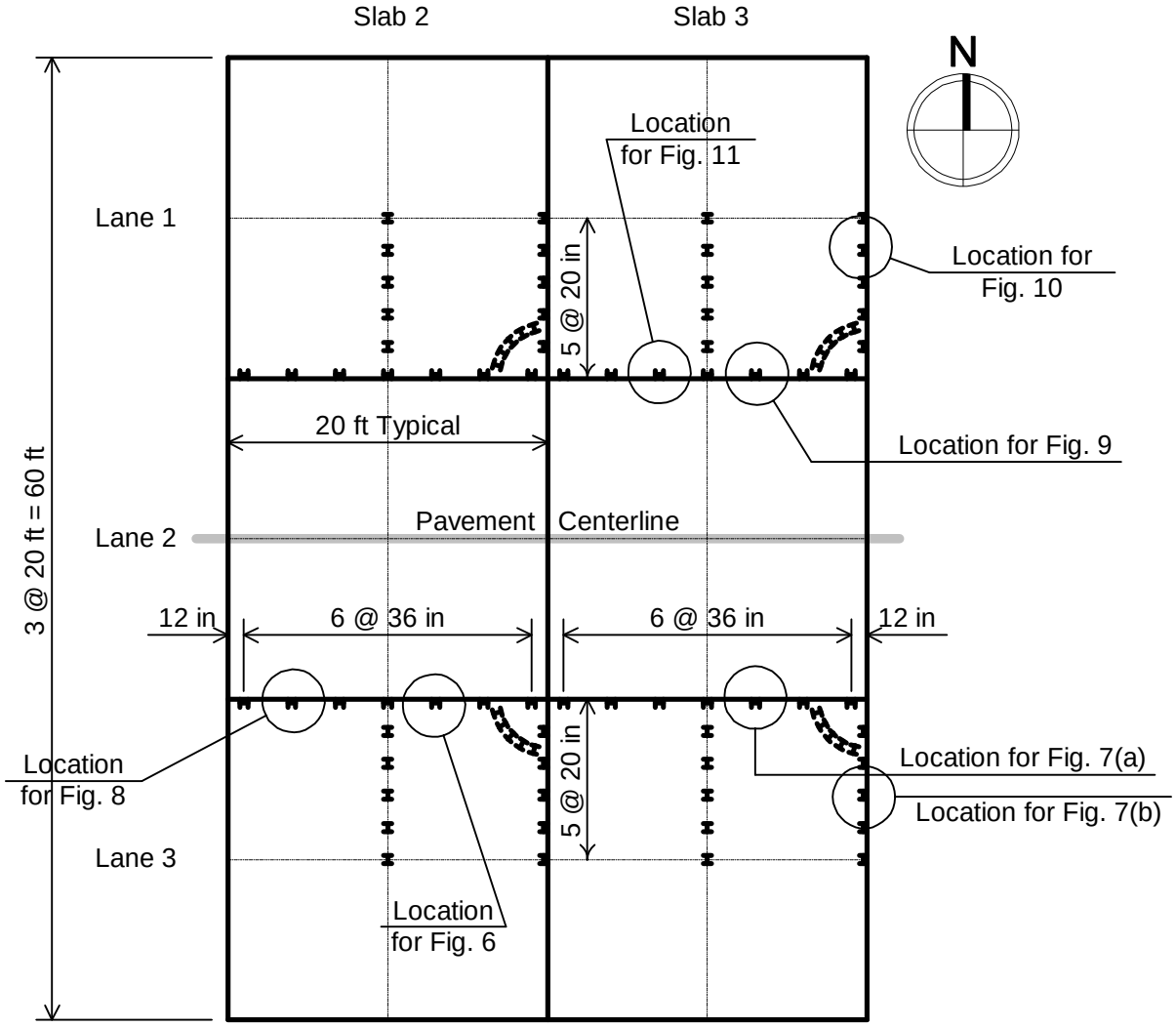

Figure 2. Locations of Concrete Strain Gages in PCC Test Item

Trafficking of the test items is in the east-west direction. The lateral position of the tires is varied to simulate vehicle wander. The load path locations (including wander) are illustrated in Figure 3. The dual wheel spacings for the four and six wheel gears were 44 and 54 inches (111.8 and 137.2 cm) respectively, and the tandem wheel spacings were 58 and 57 inches (147.3 and 144.8 cm) respectively.

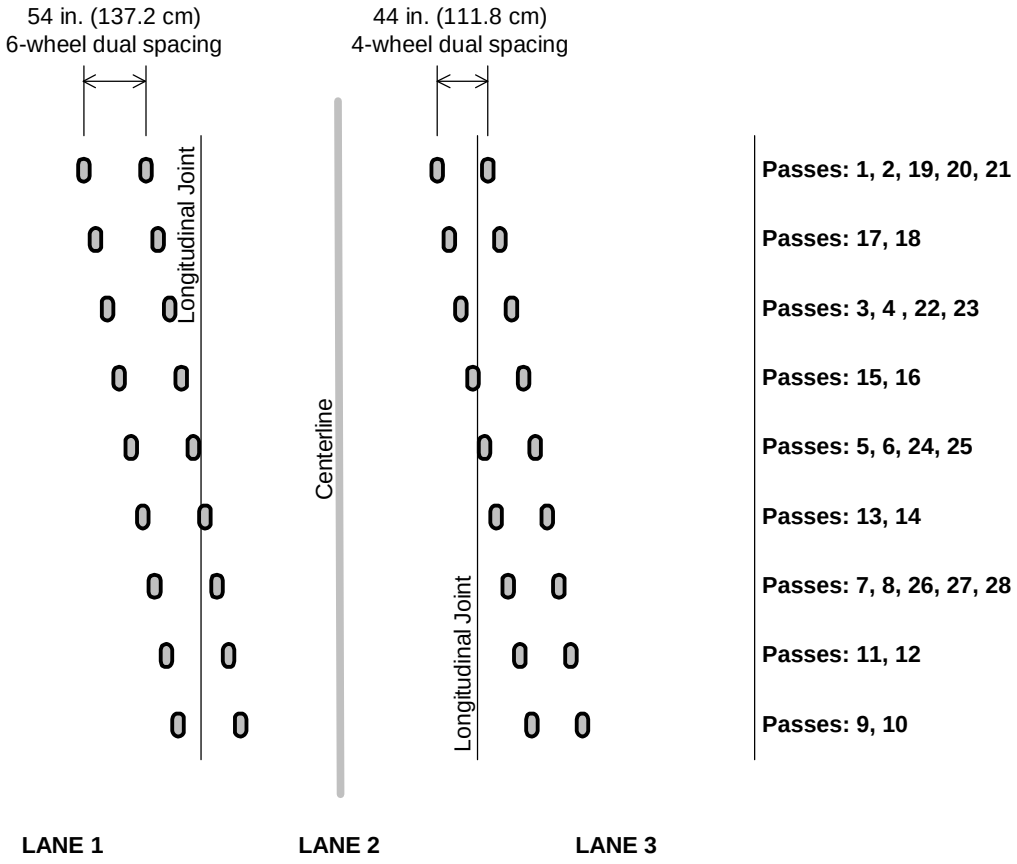

Figure 3. Carriage Locations for Traffic Tests on February 14, 2000 (28 Passes)

FAILURE MODES OBSERVED IN PAVEMENTS AT NAPTF

Twenty-eight passes of the test vehicle were applied on February 14, 2000. After completion of the initial twenty-eight passes, corner cracks were observed in test items MRS and HRS. No corner cracks were found in LRS after the first 28 passes. However, longitudinal cracks were observed in all slabs in lane 2 of LRS (except for slab 5, where the longitudinal crack was not observed until the following morning, on February 15, 2000). In March 2000, traffic tests were resumed and continued until all the slabs cracked. Ultimately, several slabs were cracked into five and even six pieces as shown in Figure 4. Corner cracks appeared in LRS during the resumed phase of testing (Figure 4c).

Figure 5 shows a typical corner cracked slab and defines the dimensions used in reporting crack size. The lengths *a* and *b* of the two sides of the cracked corners were measured and the average values are listed in Table 1. Measurements showed that the HRS slabs exhibited the largest, and the LRS slabs exhibited the smallest, corner cracks. Furthermore, it was found that

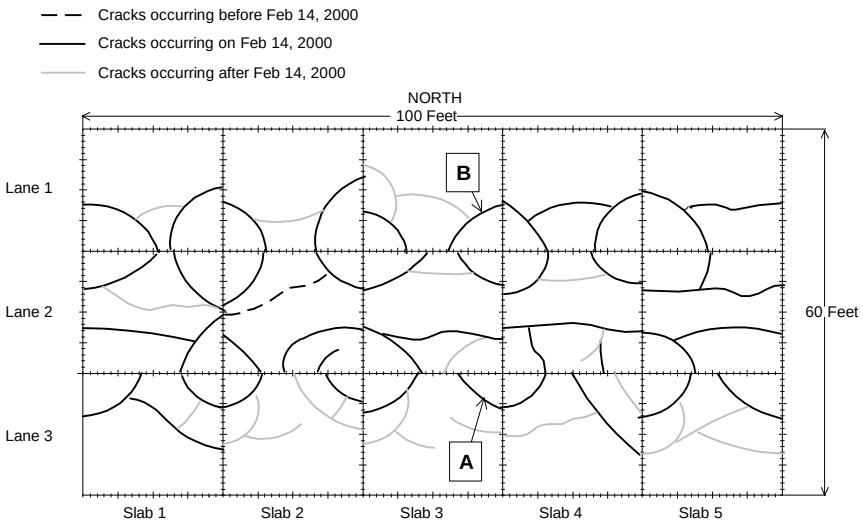

(a) Test Item HRS (after 236 passes)

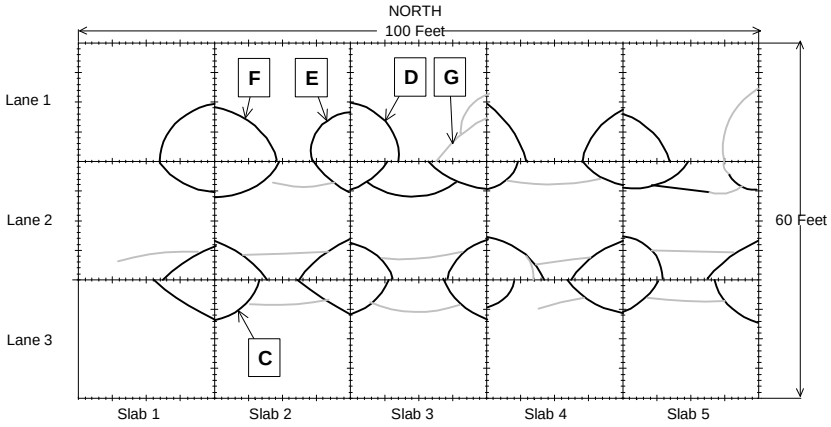

(b) Test Item MRS (after 646 passes)

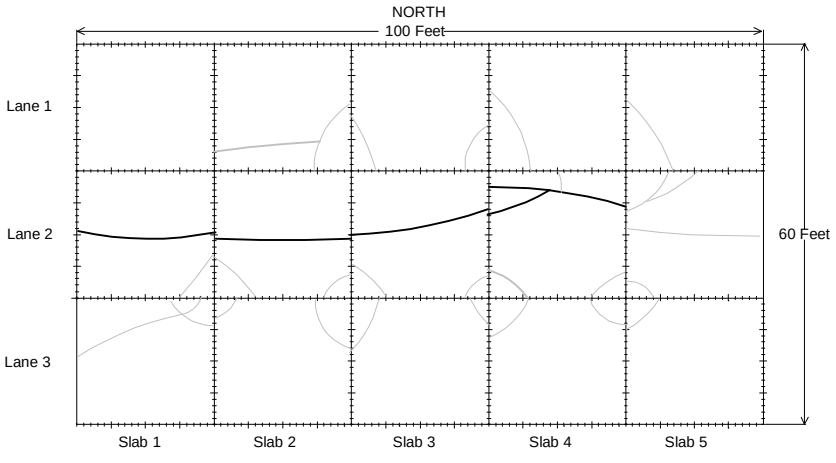

(c) Test Item LRS (after 1164 passes)

Figure 4. Pattern of Cracks Observed in Rigid Test Items

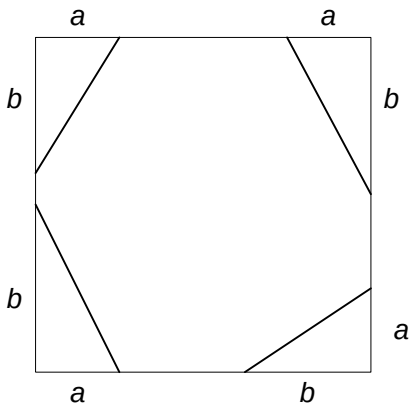

Figure 5. Definition of Corner Crack Dimensions in Table 1

Table 1. Summary of Average Crack Sizes by Test Item

	Test Item Designator		
	HRS	MRS	LRS
Average *a*, in. (cm)	78.0 (198)	72.5 (184)	54.9 (139)
Average *b*, in. (cm)	98.3 (250)	92.2 (234)	79.1 (201)

all pavement slabs were curled up at the corners, with the HRS slabs exhibiting the greatest amount of curling and the LRS slabs exhibiting the least amount of curling. The larger cracked corner areas observed on the HRS slabs are consistent with greater separation of the PCC slab corners from the econocrete base.

TYPICAL STRAIN RESPONSES (PRECRACKING)

A total of 154 concrete strain gages were installed in test items LRS, MRS, and HRS as shown in Figure 2. For each test item, four slabs were instrumented. The majority of the gages performed well. Of the total 154 concrete strain gages, 40 were found to be nonperforming, including 14 sensors (9.1%) in LRS, 12 sensors (7.7%) in MRS, and 14 sensors (9.1%) in HRS.

Sensors were installed near both the top and bottom surfaces of the slabs in order to provide measurements of the tensile and the compressive strains that develop during loading. Figures 6(a) and (b) compare the strains recorded at the top and bottom sensor positions at a slab location along the south longitudinal joint (see Figure 2). The concrete strain gage (CSG) designators are given to facilitate retrieval of strain gage data from the NAPTF database [1]. Strains plotted in Figure 6 were recorded during passes 1 and 5 of the vehicle. Figure 3 shows the lateral position of the carriage during these two passes. In both cases, one line of tires tracks exactly along the longitudinal joint line, while the other line of tires is at an offset. The difference is that for pass 5 both lines of tires are on the same side of the joint, while for pass 1 the carriage straddles the joint. Hence, for pass 1 the contribution of the second line of tires to the strain response at the sensor is reduced relative to pass 5 since only a portion of the wheel load is transferred through the longitudinal joint. This is consistent with Figure 6, which shows that the peak strains resulting from pass 1 are somewhat smaller than those resulting from pass 5.

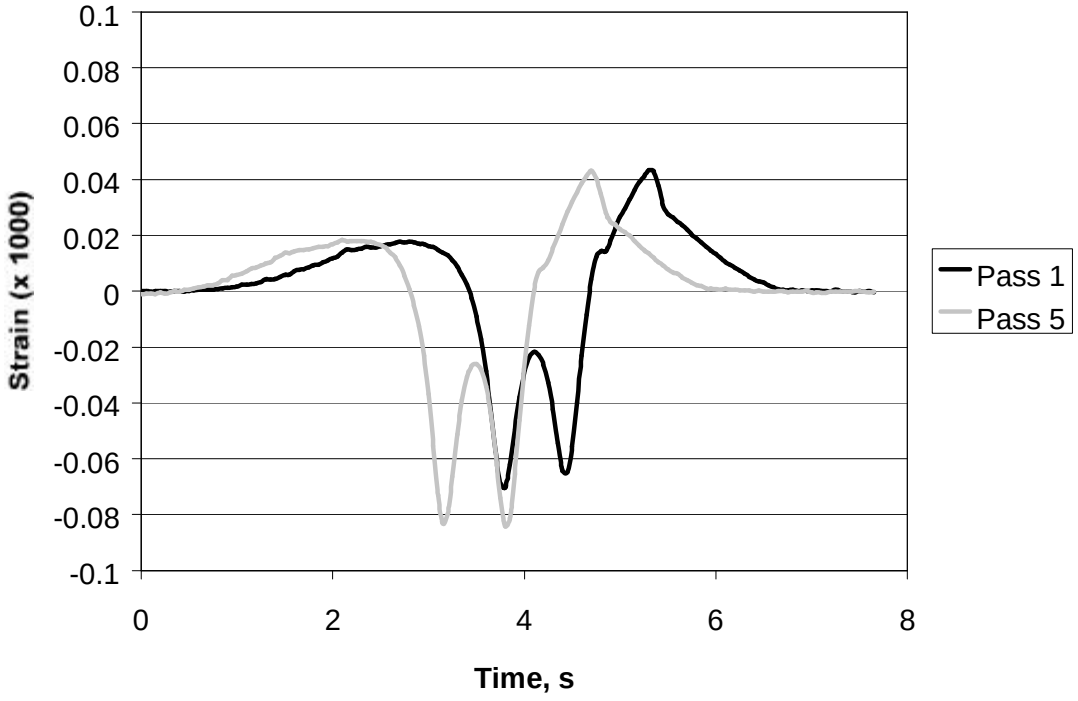

(a) Strain gage at top of slab (CSG – 303)

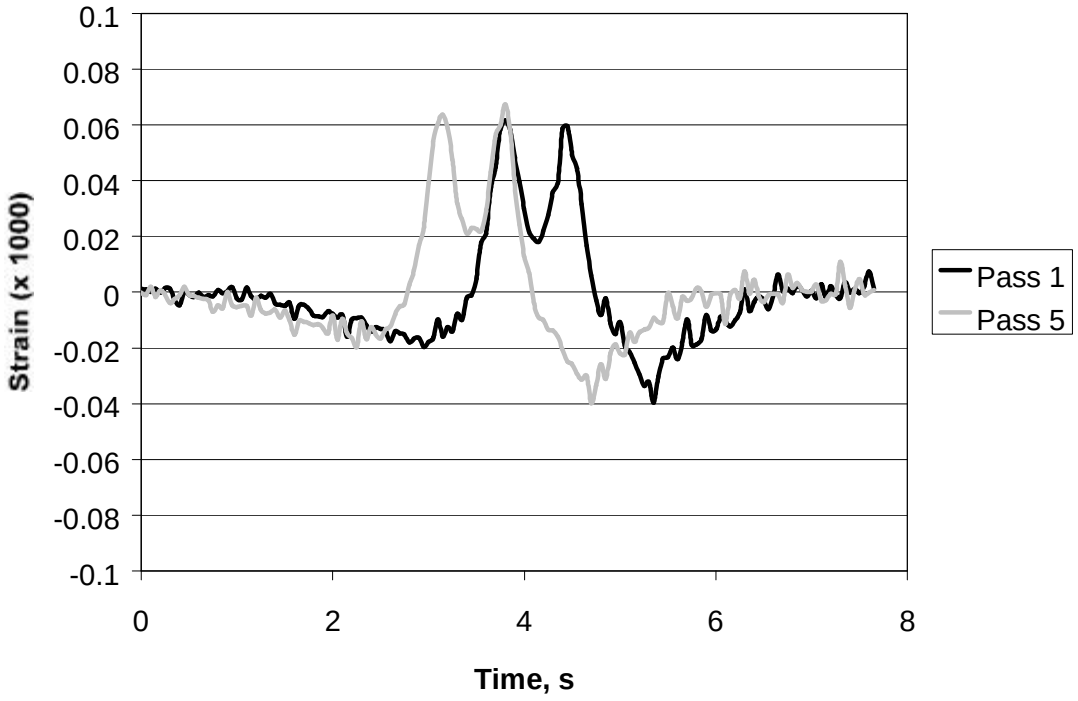

(b) Strain gage at bottom of slab (CSG – 366)

Figure 6. Typical Strain Responses in Test Item LRS for Loading of the South Longitudinal Joint (Four-tire Load)

ANALYSIS OF SLAB CRACKING DURING INITIAL TRAFFICKING (FOUR-TIRE LOAD)

Figure 7 gives evidence of when and how the corner crack,` indicated by "A" in Figure 4(a), developed.

–

Gages CSG – 173 (top) and CSG – 192 (bottom) displayed unusually high strain readings attributed to cracking through the strain gage location. The high strain values for pass 1 are consistent with large displacements associated with slab cracking. For example, the peak strain value recorded for pass 1 is 0.22×10^{-3} (Figure 7b). This is a tensile strain measured near the top of the slab at the transverse joint location. For comparison, if the modulus of elasticity of the concrete is estimated as 6,000,000 psi (41,370 MPa), and the actual concrete flexural strength is estimated conservatively as 1000 psi (6.89 MPa), then the tensile strain at the gage depth needed to cause rupture of the concrete is

$$\frac{1{,}000\ \text{psi}}{6{,}000{,}000\ \text{psi}} \times \left(\frac{3}{4.5} \right) = 0.11 \times 10^{-3}$$

or about half of the actual recorded strain at the gage. The factor $(3/4.5)$ in the above calculation is needed to adjust for the difference between the 1½ in. (3.8 cm) embedded depth of the sensor and the extreme fiber (top surface) of the slab. Based on the above analysis, it was verified that crack A in Figure 4(a) initiated near the longitudinal joint and extended through the slab to the transverse joint during the first pass of the vehicle. Similar analyses showed that the majority of corner cracks identified in HRS lane 3 also developed during the first vehicle pass.

Figure 8 compares strain measurements in test item MRS for a pair of strain gages (CSG – 473, bottom, and CSG – 474, top) located at a point along the south longitudinal joint as indicated in Figure 2. The corner crack at location C in Figure 4(b) occurred during pass 1, as indicated by the sharp change in the shape of the tensile strain response at 4.2 s of pass 1 (Figure 8a). Similar analyses of the other strain gages in MRS confirm that, as with HRS, the majority of corner cracks developed during the first or second pass of the vehicle. It is instructive to compare the strain readings in Figure 8 with the LRS strain curves in Figure 6, also recorded during passes 1 and 5. It was observed that for Figure 6 (LRS), the strains for pass 5 were higher than those for pass 1 due to the positive contribution of the interior line of tires. By contrast, in Figure 8 (MRS) the response for pass 5 is much smaller than that for pass 1. In the latter case, the contribution of the two interior wheels did not increase the response, simply because corner crack C had already formed prior to pass 5.

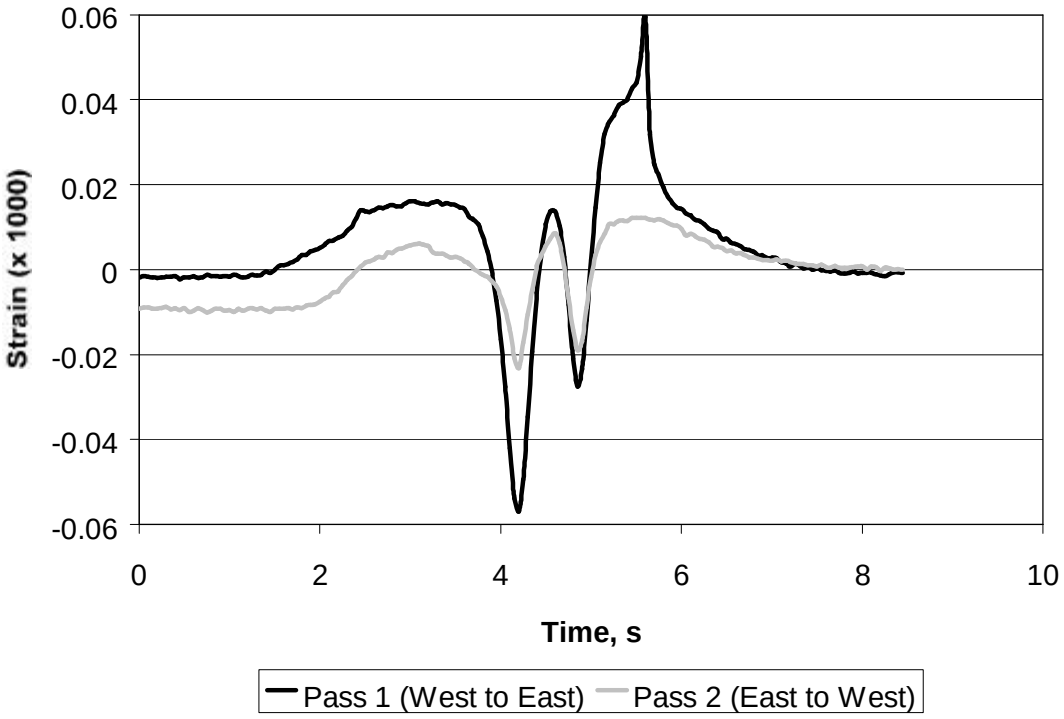

(a) Strain gage at top of slab, longitudinal joint (CSG – 109)

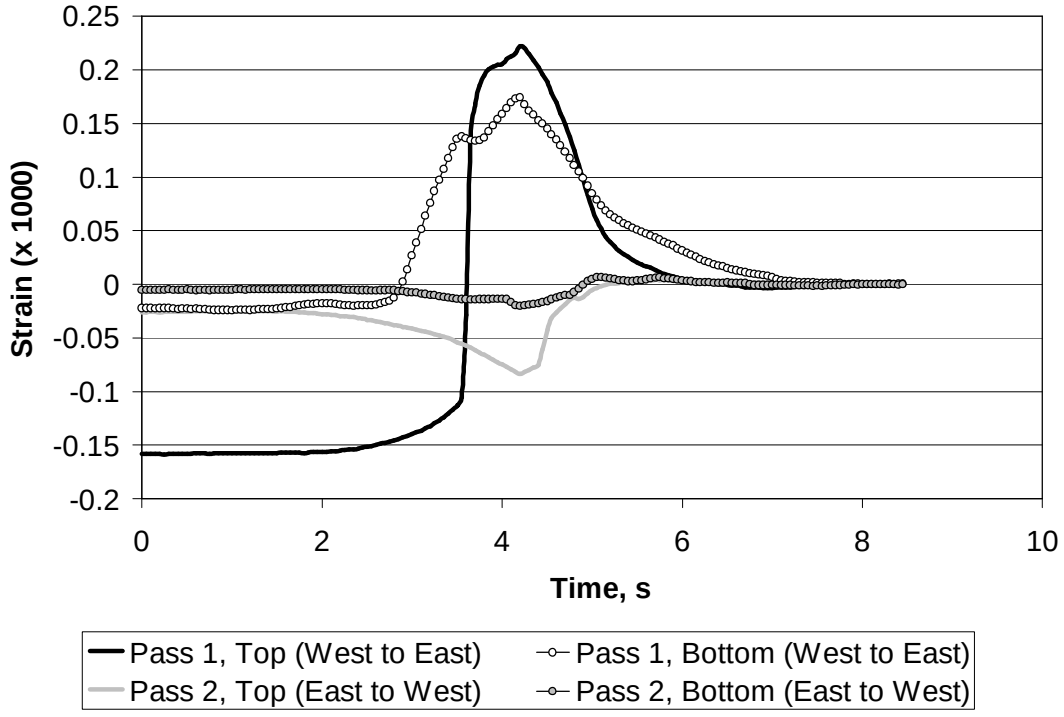

(c) Strain gages at top (CSG –173) and bottom (CSG – 192) of slab, transverse joint

Figure 7. Strain Responses in Test Item HRS, Lane 3 (Four-tire Load). Strain responses show evidence of crack formation at the slab corner identified by "A" in Figure 4(a)

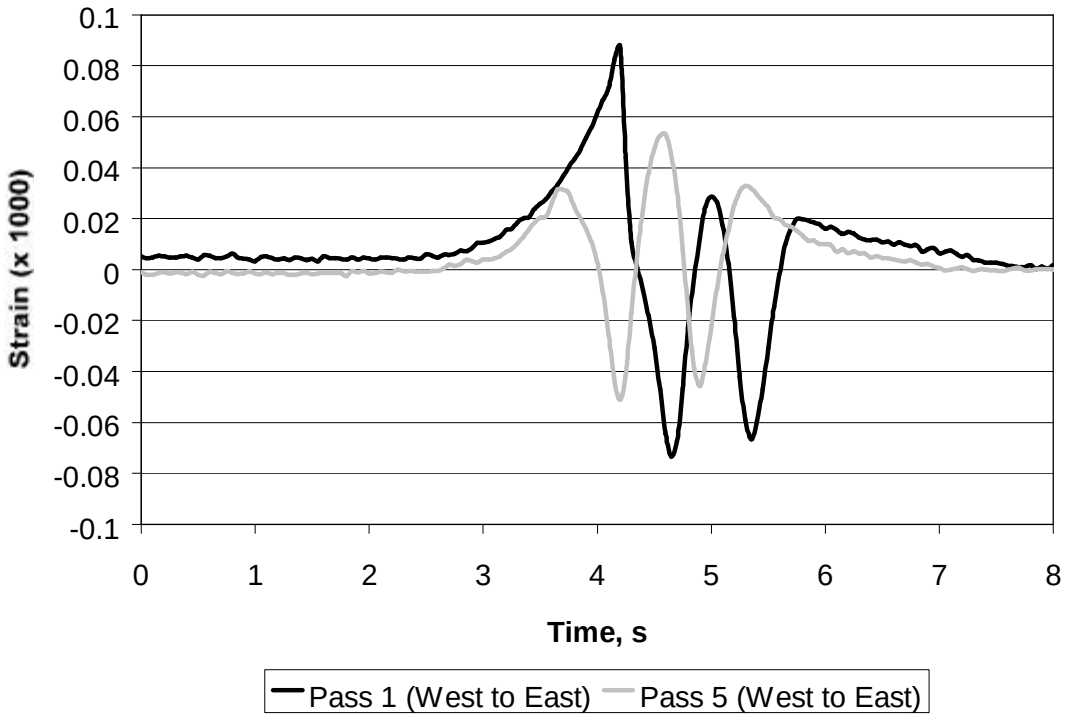

(a) Strain gage at top of slab (CSG – 474)

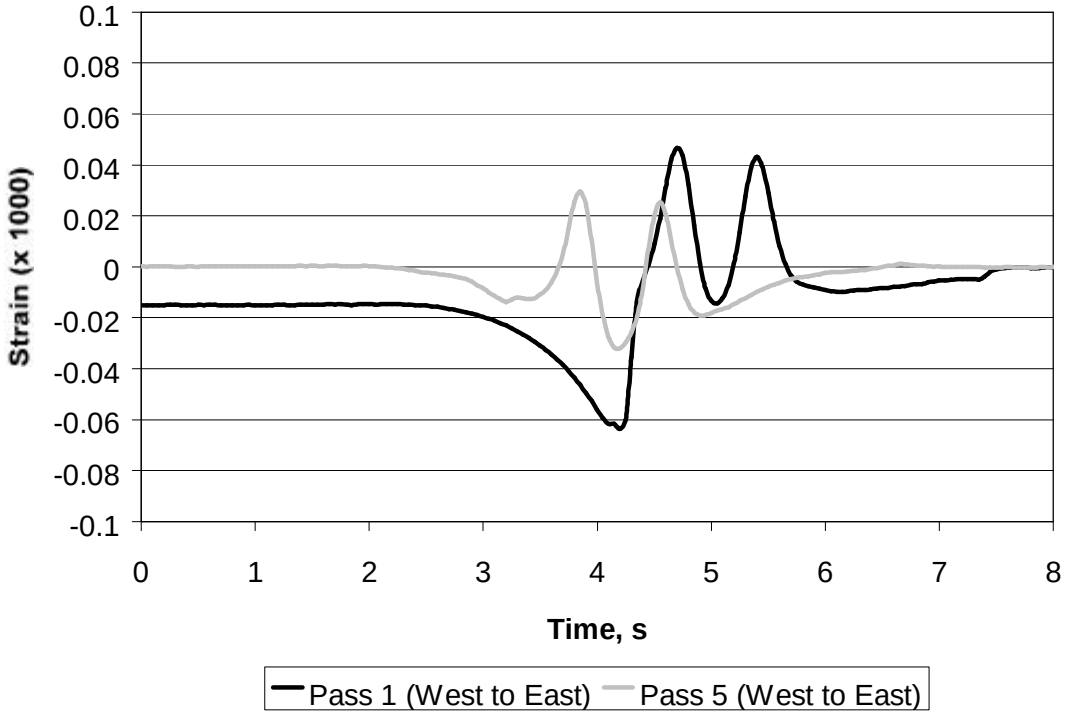

(b) Strain gage at bottom of slab (CSG – 473)

Figure 8. Strain Responses in Test Item MRS, Lane 3 (Four-tire Load). Strain responses show evidence of crack formation at the slab corner identified by "C" in Figure 4(b)

ANALYSIS OF SLAB CRACKING DURING INITIAL TRAFFICKING (SIX-WHEEL LOAD)

Figure 9 shows selected strain time histories for a strain gage (CSG-50) located along the north longitudinal joint in test item HRS. This sensor is located near crack B as shown in Figure 4(a). Four curves are presented: two for traffic in the west-to-east direction (Figure 9a) and two for traffic in the east-to-west direction (Figure 9b). All four curves are based on the same gear lateral position, with one line of tires in the six-wheel carriage tracking closely along the longitudinal joint (see Figure 3). Taken together, the four curves suggest that corner crack B developed after pass 6 but before pass 24. The strain histories for passes 24 and 25 are highly degraded in comparison with the corresponding strain histories for passes 5 and 6, which is consistent with the probable cracked condition of the slab during the later passes. That cracking did not occur at this location prior to or during pass 5 is clear because pass 6 essentially duplicated (in reverse) the strain history associated with pass 5, indicating that the slab still had structural integrity.

As shown in Figure 4(a), corner crack C extends from the longitudinal joint to the transverse joint in lane 1. Figure 10 presents selected strain records for the strain gage (CSG-12) at the approximate location where crack C intersects the transverse joint. Strain records are shown for four consecutive passes of the vehicle, passes 9 through 12. Based on analysis of these strain records, it is believed that crack B initiated at the transverse joint during pass 10 (maximum strain developed in Figure 10) and was extended continuously during subsequent passes 11 and 12. It is believed that the crack progressed from the transverse joint toward the longitudinal joint during this loading phase. Similar analyses of other strain records in lane 1 of test item HRS (six-wheel load) indicate that all cracks in that area started after pass 9.

A somewhat different situation was observed in lane 1 of test item MRS. On February 14, 2001, after the initial 28 vehicle passes, all slab corners in MRS along both longitudinal joints were observed to be cracked except for one corner (identified by G in Figure 4b). The corner crack (D) that appeared in the southwest corner of slab 3 crossed through strain gage CSG-156 (Figure 2), so it is reasonable to expect that the strains recorded by CSG-156 provide useful information about the cracking history of this slab. Figure 11 shows three strain records for CSG-156. The very large disparity in the magnitudes of the strains between passes 5 and 24 suggests that it was between those two passes that cracking initially occurred. It is interesting to note that the magnitudes of the peak strains recorded for passes 24 and 25 are far beyond the elastic range. Nevertheless, even in the postcracking environment the shapes of the strain curves are intelligible, and the peaks corresponding to the passage of each of the three tires can be identified readily.

Since no strain gage exists on slab 3` at the location where crack D intersects the transverse joint, it is impossible to determine from the available information whether this crack initiated at the transverse or at the longitudinal joint. Crack D might have initiated from the longitudinal joint side during pass 6, or alternatively, from the transverse joint during either pass 9 or pass 10. Either possibility is consistent with the data in Figure 11 and other strain records.

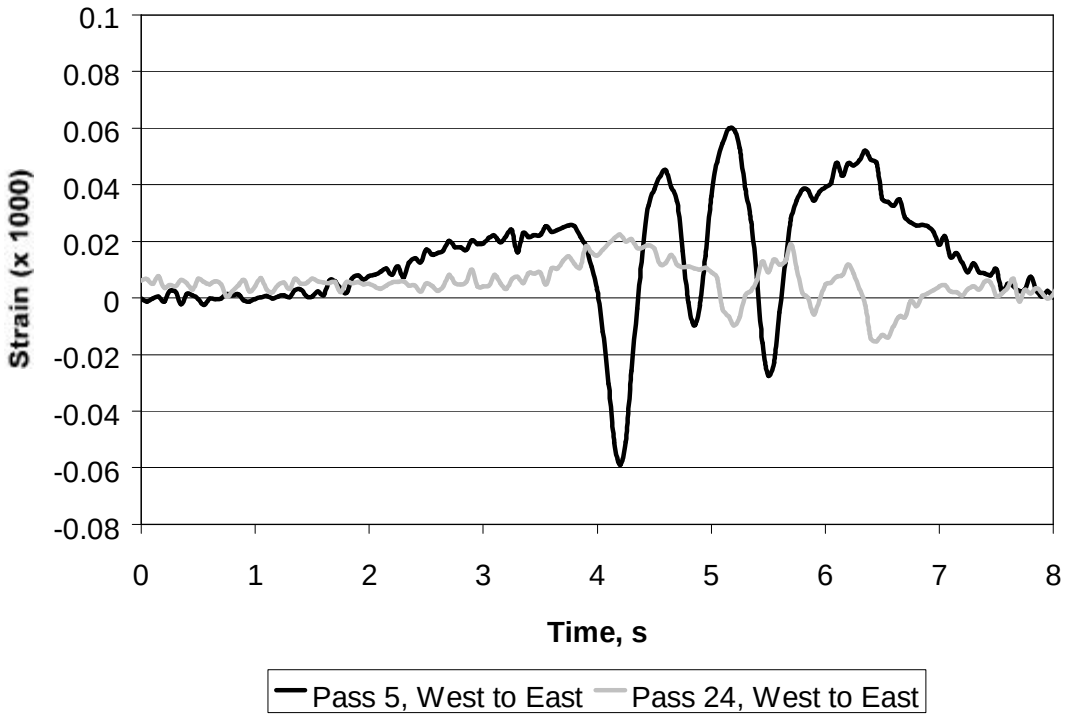

(a) Strain gage at top of slab, west to east traffic (CSG-50)

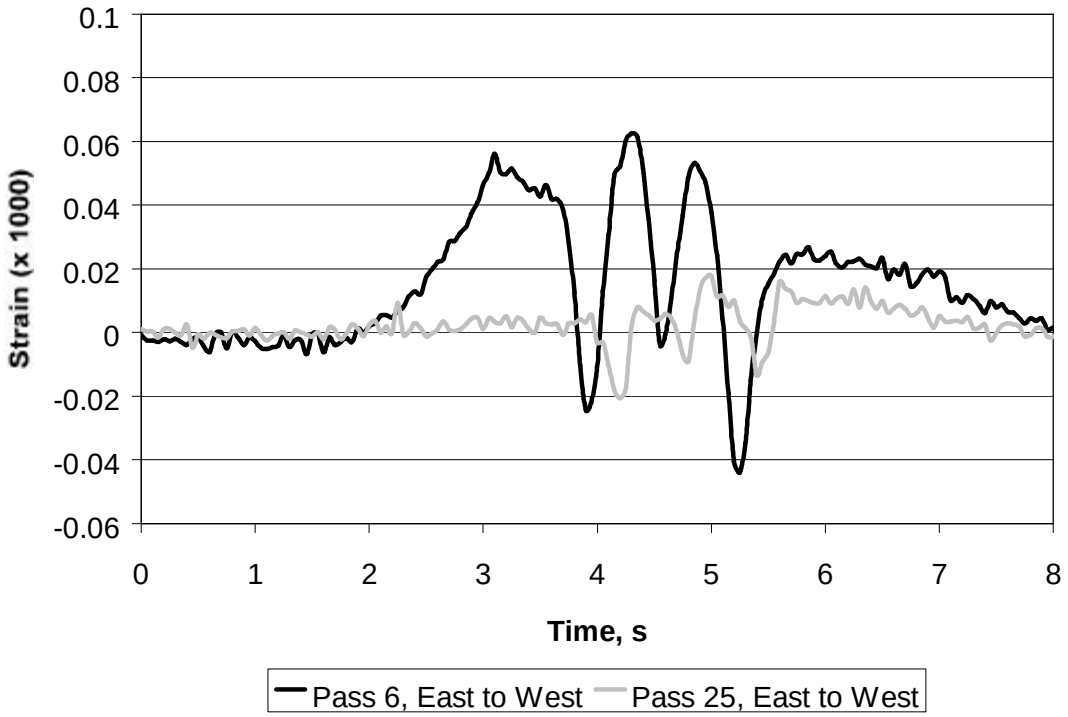

(b) Strain gage at top of slab, east to west traffic (CSG-50)

Figure 9. Strain Responses in Test Item HRS, Lane 1 (Six-tire Load)

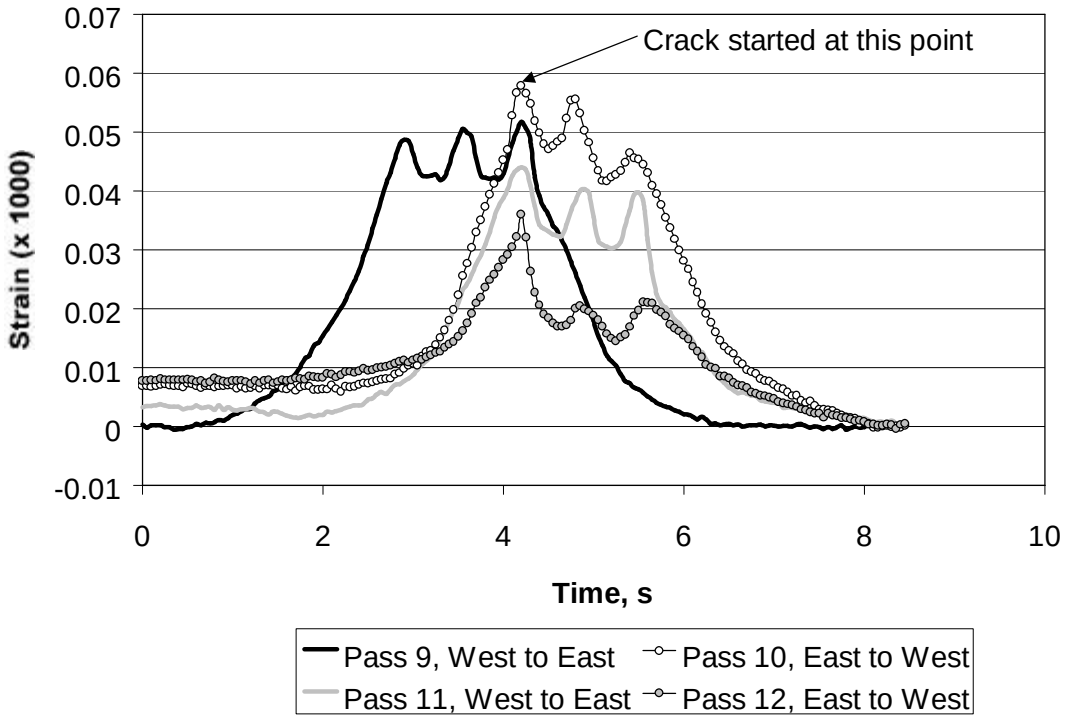

Figure 10. Strain Responses in Test Item HRS, Lane 1 (Six-tire Load). Strain gage at top of slab (CSG-12)

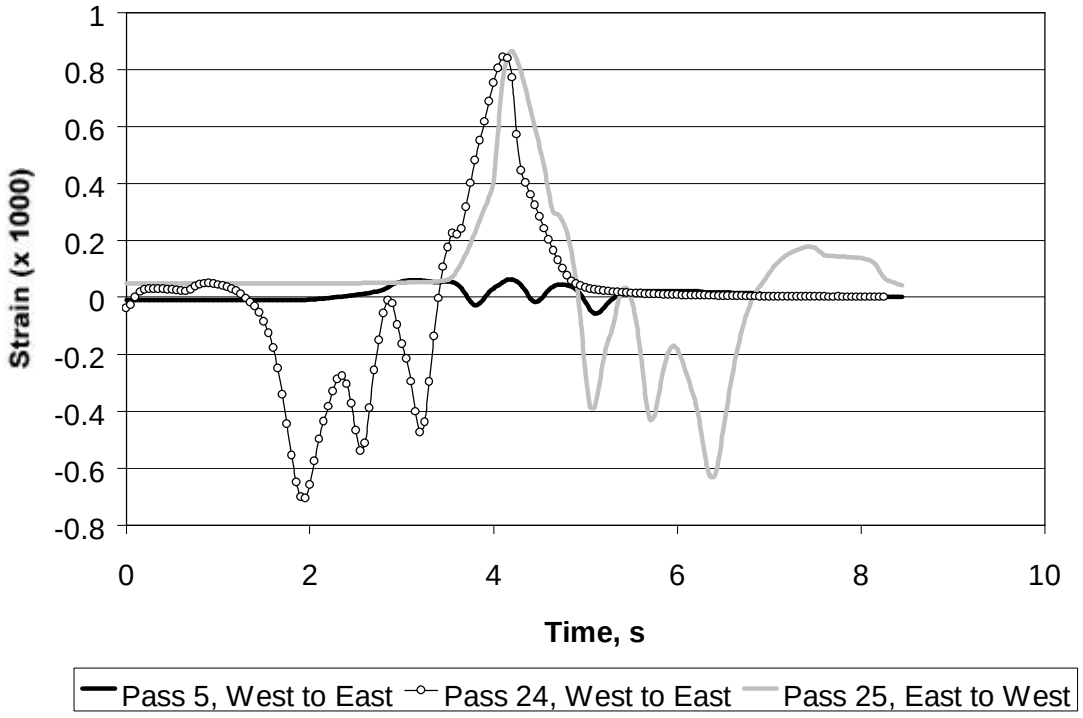

Figure 11. Strain Responses in Test Item MRS, Lane 1 (Six-tire Load). Strain gage at top of slab (CSG-156)

CONCLUSIONS

The measured pavement strains in the National Airport Pavement Test Facility (NAPTF) rigid pavement test items contain significant information that is useful for understanding slab behavior under simulated aircraft traffic loading. In particular, the numerous concrete strain gages installed in the test items enabled researchers at the Federal Aviation Administration Airport Technology Research and Development Branch to analyze corner cracks that typically appeared during initial traffic testing. Only a small portion of the data collected to date has been analyzed and presented in this paper. Static and dynamic data including strain gage data files are available for download through the NAPTF's searchable online database [1].

Examples of strain gage records presented in this paper demonstrate the need for detailed visual surveys and crack mapping to supplement basic strain data. Many of the strain gage responses reported in this paper could not have been interpreted properly, except in light of the supplemental cracking information obtained from the visual survey.

ACKNOWLEDGEMENT

The work described in this paper was supported by the FAA Airport Technology R&D Branch, Dr. Satish K. Agrawal, Manager. Special thanks are also given to Mr. Hector Daiutolo of Galaxy Scientific Corporation for carefully reviewing the paper. The contents of the paper reflect the views of the authors, who are responsible for the facts and accuracy of the data presented within. The contents do not necessarily reflect the official views and policies of the FAA. The paper does not constitute a standard, specification, or regulation.

REFERENCES

1. FAA (2001) National Airport Pavement Test Facility Database. Internet site: **http://www.airporttech.tc.faa.gov/naptf/**